# 25.4 DEPENDENCE OF HURRICANE INTENSITY AND STRUCTURES ON VERTICAL RESOLUTION

Da-Lin Zhang and Xiaoxue Wang
Department of Meteorology, University of Maryland, College Park, MD 20742

## 1. Introduction

Rapid growth in computing power has recently allowed us to use small horizontal grid length, even down to 1 – 2 km, to model the inner structures and evolution of various mesoscale convective systems (MCSs). Indeed, increasing horizontal resolution with better model physical parameterizations has shown significant improvements in the quality of numerical weather prediction (NWP). However, the adequacy of vertical resolution in the current NWP models has recently been questioned, and some studies indicated that increasing horizontal resolution alone does not always guarantee a better solution, particularly in the presence of phase changes.

For example, Lindzen and Fox-Rabinovitz (1989) derived a consistency criterion between horizontal and vertical resolution for quasi-geostrophic flows. They pointed out that a fine horizontal resolution, without considering an appropriate vertical resolution, would lead to the production of 'noisy' fields and may degrade the overall accuracy of the solution. Based on a two-dimensional hydrostatic primitive equation model, Pecnick and Keyser (1989) derived a relationship that physically relates horizontal scales to vertical scales of an upper-level frontal structure. In contrast to the above results that were obtained with dry dynamics equations, Persson and Warner (1991) studied the resolution consistency in a hydrostatic (moist) simulation of conditional symmetric instability associated with frontal rainbands, and noted the development of spurious gravity waves when the vertical and horizontal resolutions are not consistent.

The purpose of this study is to examine the sensitivity of explicit simulation of Hurricane Andrew (1992) to varying vertical resolutions in terms of its intensity and inner-core structures. Liu et al. (1997; 1999) have shown a 72-h successful simulation of the hurricane track and intensity, as well as the structures of the eye, the eyewall, spiral rainbands, the radius of maximum winds (RMW), and other inner-core features as compared to available observations and the results of previous hurricane studies. In this study, the model set-ups, such as the model domains, grid sizes, initial conditions and physics options, are the same as those used by Liu et al. (1997), except for the vertical resolution. The next section describes briefly the numerical model used for this study and experimental design. Section 3 shows sensitivity simulations, respectively. A summary and conclusions are given in the final section.

## 2. Experiment design

In the present study, a two-way interactive, movable, triply-nested, cloud-resolving, non-hydrostatic version of the Pennsylvania State University/National Center for Atmospheric Research (PSU/NCAR) mesoscale model (MM5; see Dudhia 1993) is used. The triply nested domains have the (x, y) dimensions of 82 x 64, 124 x 94 and 124 x 94 with the grid sizes of 54, 18 and 6 km, respectively. The model physics include (i) the Tao-Simpson (1993) cloud microphysics scheme for the 6-km grid mesh, (ii) the Blackadar planetary boundary layer (PBL) parameterization (Zhang and Anthes 1982) and (iii) a cloud-radiation interaction scheme (Dudhia 1989). The sea-surface temperatures (SST) are held as constant in time during the 72-h integration. The model is initialized at 1200 UTC 21 August 1992 with a bogussed hurricane vortex. See Liu et al. (1997) for more details.

In their simulation of Hurricane Andrew (1992), Liu et al (1997) used 23 vertical $\sigma$ layers. For the present study, we define a control run, in which 46 uneven half-$\sigma$ levels with higher resolution in the PBL are used (Exp. CTL46). Several sensitivity experiments are designed to study the effects of varying vertical resolutions on the simulated hurricane intensity and inner-core structures. In Exp. HRL69, 23 vertical layers are evenly added to CTL46, whereas in Exp. LRL23 the CTL46 vertical resolution is halved evenly. In addition, another three sensitivity experiments are conducted to examine the effects of varying vertical resolutions in different portions of the troposphere on the hurricane intensity and structures: (i) use the same vertical resolution as that in Exp. CTL46 above the melting level (roughly at $\sigma$ = 0.44) but keeping the same resolution as that in Exp. LRL23 for the layers below (Exp. HUT35, i.e., higher resolution in the upper troposphere); (ii) use the same vertical resolution as that in Exp. CTL46 below the melting level but keeping the same resolution as that in Exp. LRL23 for the layers above (Exp. HLT35, i.e., higher resolution in the lower troposphere).

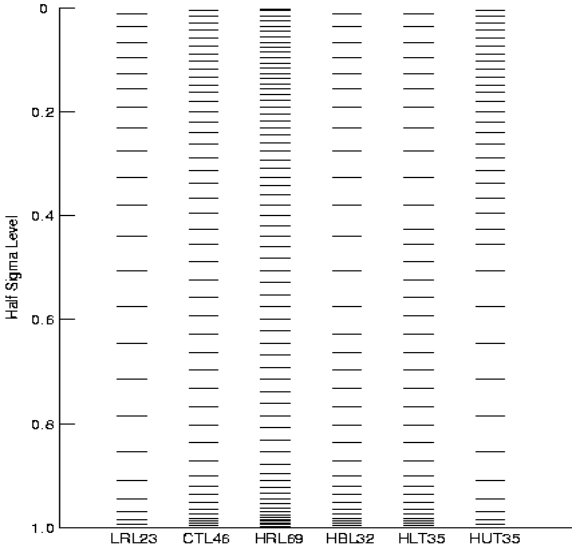


Fig. 1: Vertical distribution of half-$\sigma$ levels for each sensitivity experiment. Dashed lines denote roughly the location of melting layer.

and (iii) double the vertical resolution in the lowest 150 hPa layer, i.e., up to $\sigma$ = 0.845 (Exp. HBL29). Fig. 1 illustrates the distribution of the vertical $\sigma$-layers for all sensitivity simulations. In the above sensitivity simulations, all of the other model parameters are kept the same as those in Exp. CTL46. See Zhang and Wang (2003) for more details.

It should be mentioned that based on the resolution consistency criterion (1), the vertical resolution for a grid size of 6 km should be about 60 m. Clearly, the highest vertical resolution used herein (i.e., Exp. HRL69) is still much coarser than that theoretically required, but it has already pushed the existing computing power into the limit. Thus, our study will be limited to the highest vertical resolution possible with the current computing resources that are available to us.

## 3. Results

In this section, we investigate the impact of varying vertical resolutions and time-step sizes on the simulation of Hurricane Andrew (1992) in terms of its intensity, eyewall structures and heating profiles.

Fig. 2 compares the time series of the simulated minimum central pressures from the resolution sensitivity experiments. Note first that the simulated hurricane intensities depart more significantly with time between different experiments; the maximum intensities could range from the deepest 899 hPa in Exp. HRL69, to 907 hPa in Exp. CTL46 and the weakest 932 hPa in Exp. HUT35. The time series of central pressure from Exps. LRL23 and HRL69 are almost symmetrically distributed above and below that of Exp. CTL46, respectively, with the difference as large as 33 hPa in the first 60-h integration.

Second, increasing the vertical resolution in the low troposphere (HLT35) from LRL23 yields an intensity time series similar to that of HRL69, only a few hPa weaker in the first 60-h integration, implying the significant effects of changing the lower-

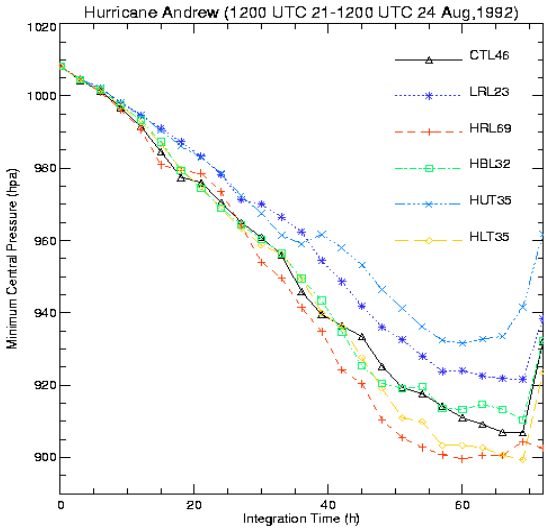


Fig. 2: Three hourly time series of the minimum central pressure from all sensitivity experiments.

level vertical resolution on the intensity prediction. Of interest is that increasing the upper-level vertical resolution (HUT35) from LRL23 even produces the weakest storm, i.e., 14 hPa weaker than that in LRL23, despite the use of more vertical layers. Of further interest is that the HUT35 time series follows closely that of LRL23 during the first 30-h integration, deepens slightly from 30 – 36 h, but becomes 10-20 hPa weaker than the LRL23 storm afterward. An examination of the model-simulated radar reflectivity maps reveals that this bifurcation is caused by different cloud structures in the eyewall and spiral rainbands as a result of different vertical resolutions. For example, the model generates a partial eyewall in HUT35, but a near-full eyewall in Exp. LRL23 with marked differences in size and rainband distribution from the 39-h integration, which is just a couple of hours before the crossover of the sea-level pressure time series (cf. Figs. 2 and 3). Similarly, the time series in Exps. HLT35 and HBL29 are similar to that of CTL46 in the first 36 h, but then both become significantly deeper. Despite the use of less vertical layers in HLT35 and HBL29, their final intensities are close to the intensity in HRL69. The results suggest that (i) increasing the vertical resolution in the lower troposphere is more efficient than that in the upper levels in deepening a hurricane, and (ii) different partitioning of a given number of vertical layers could have different impact on the deepening rates and cloud structures in the eyewall and rainbands during the different stages of hurricane development.

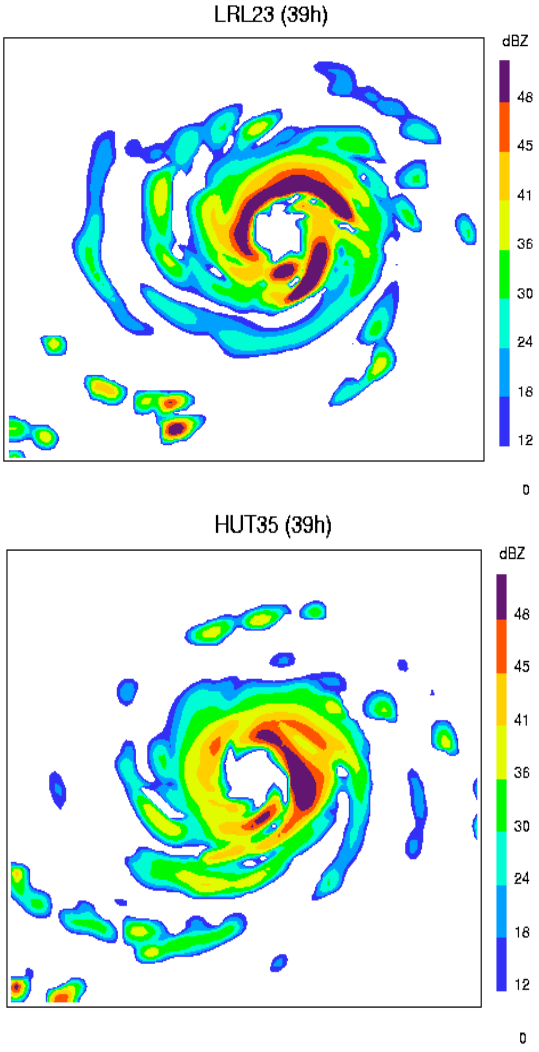


Fig. 3: Horizontal distribution of radar reflectivity, taken at □ □ 0.785 (i.e., near 800 hPa), from the 39-h integration for (a) Exp. LRL23; and (b) Exp. HUT35.

The time series of simulated maximum surface winds, given in Fig. 4, shows the relation of the simulated hurricane intensity to the surface layer resolution and frictional effects. The use of the thickest surface layer

(80 m – at a full-□ level) in Exp. LRL23 produces the greatest maximum surface wind of 75 m $s^{-1}$ prior to landfall, whereas the thinnest surface layer (about 27 m) in HRL69 has the weakest maximum surface wind of 63 m $s^{-1}$ in spite of its deepest minimum pressure (cf. Figs. 2 and 4). This is consistent with the notion that the frictional effects would be more (less) pronounced if a thinner (thicker) surface layer of air mass interacts with the bottom surface.

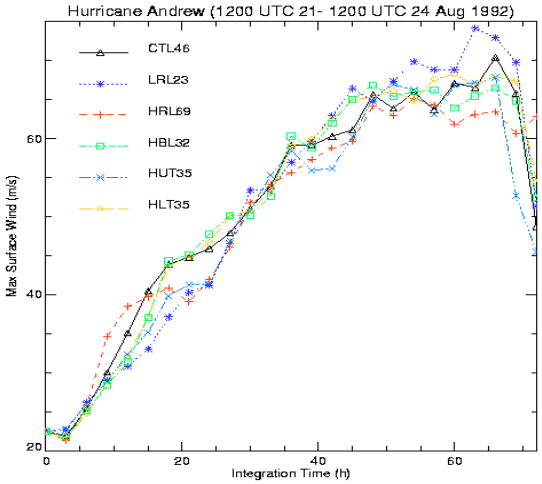


Fig. 4: As in Fig. 2, but for the maximum surface winds.

The simulated radar reflectivity from the 54-h integrations shows different inner-core structures of clouds and precipitation among the various experiments (see Fig. 5). It is evident that the eyewall convection becomes more intense, more compact and more symmetric with a wider annulus of clouds outside as the vertical resolution increases from 23 to 69 layers. Different inner-core cloud/precipitation structures also appear in the other three sensitivity runs. For example, the eyewall convection in HBL29 is also near-symmetric with more convection occurring to the west, whereas there is a tendency to develop a partial double eyewall to the east in HLT35 (not shown), as also hinted from Fig. 2. Surface rainfall amounts and distribution, including major spiral rainbands, also differ between the simulations (not shown). These results are all consistent with the simulated intensity changes, as expected.

Fig. 6 display the height-radius cross sections of vertical motion superposed with the in-plane flow vectors from the 54-h integration. These maps exhibit a typical hurricane structure: an intense radial inflow in the PBL, an outflow jet near the top of the PBL where the tangential winds are peaked, a slantwise updraft with a negative shear in horizontal winds in the eyewall, and an outflow layer in the upper troposphere. In general, the sensitivity of the simulated flow intensity to vertical resolution is consistent with that of the minimum central pressure. For instance, increasing the upper-level resolution (HUT35) has less notable impact on the height-radius distribution of horizontal winds and vertical motion, as compared to LRL23. On the other hand, increasing the low-level resolution (i.e., HBL29 or HLT35) generates the amplitudes of the low-level horizontal wind that are similar to those in CTL46, as expected. However, despite the development of a more intense storm in HBL29 (and HLT35), its associated upper-level outflows are similar to those in LRL23 but markedly weaker than those in CTL46. This indicates the importance of designing a comparable distribution of vertical resolution in studying hurricanes' inner-core structures. Better results tend to be obtained when high-resolution layers are used throughout the troposphere.

When properly designed, increasing vertical resolution tends to increase the magnitude of vertical motion, for example, the maximum updraft varies from 2.5 m $s^{-1}$ in LRL23 to 4.5 m $s^{-1}$ in HRL69. Doubling the low-level resolution (HBL29 and HLT35) can also duplicate somewhat the eyewall structure and intensity shown in higher resolution runs (e.g., CTL46). Again, doubling the upper-level resolution (HUT35) from LRL23 affects little the vertical structure and amplitude of vertical motion in the secondary peak updraft, corresponding to the peak tangential wind and an outflow

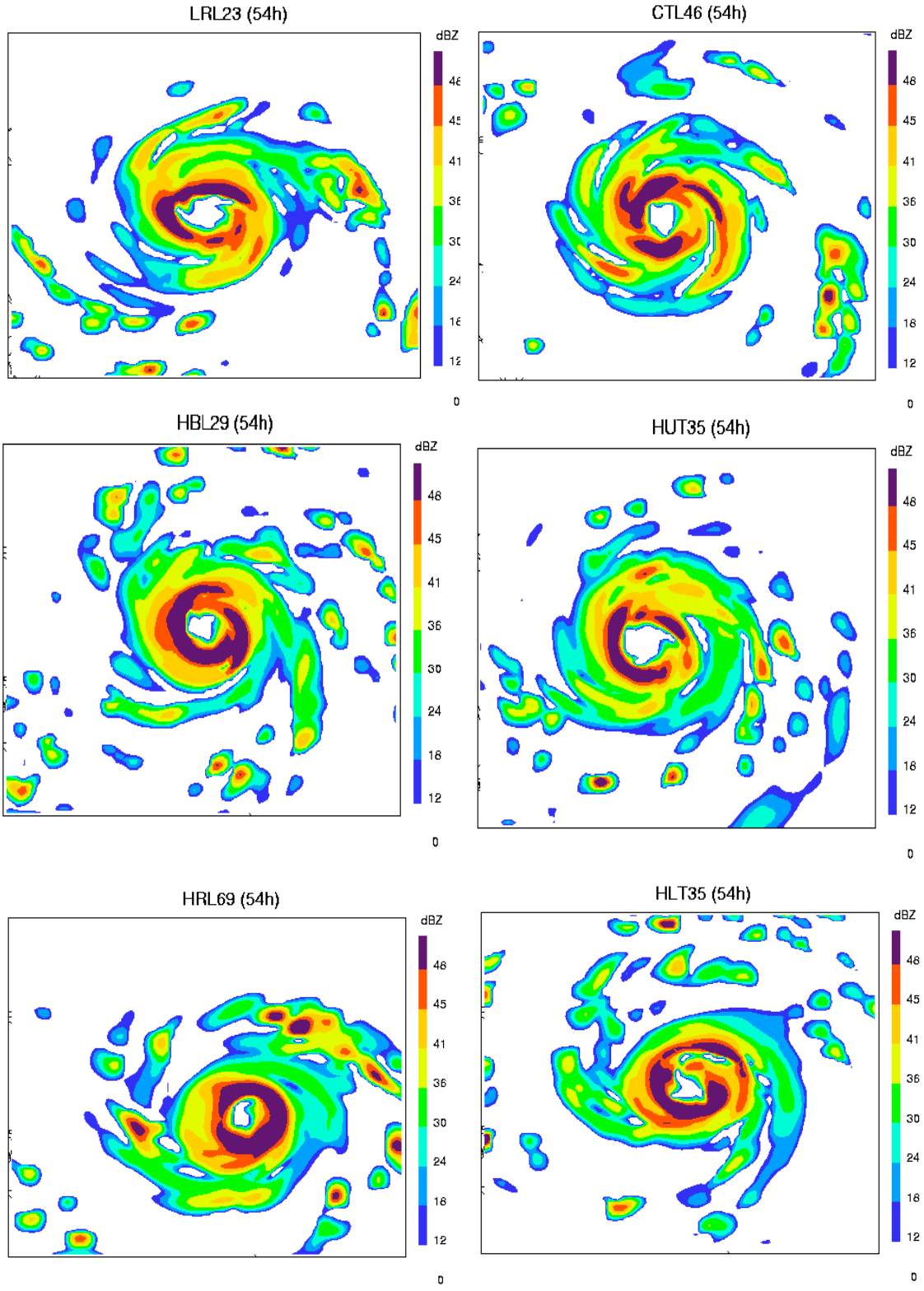


Fig. 5: Horizontal distribution of radar reflectivity, taken at □ □ 0.785 (i.e., near 800 hPa), from the 54-h integrations of all sensitivity experiments.

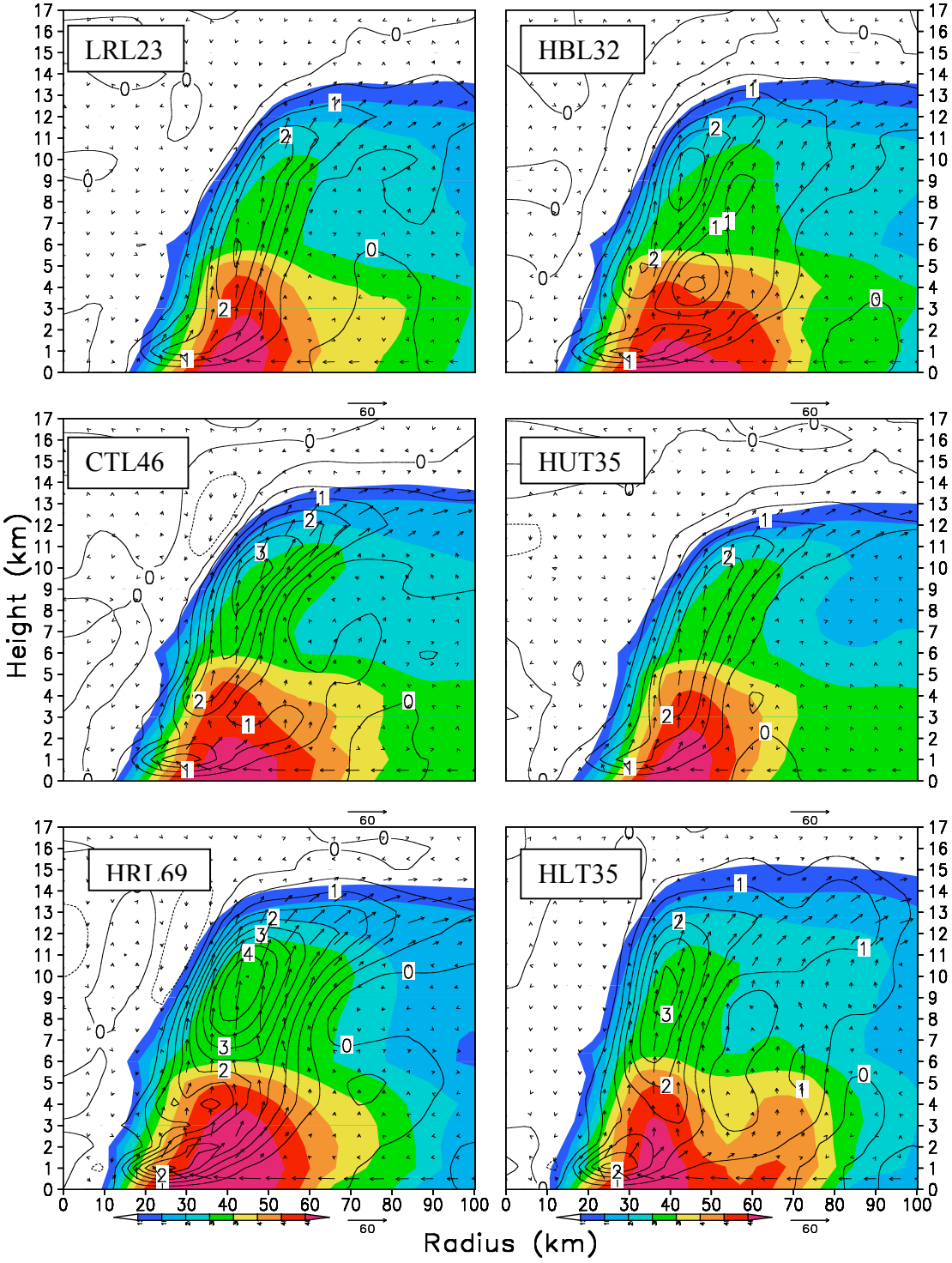


Fig. 6: Height-radius cross sections of vertical velocity, at intervals of 0.5 m $s^{-1}$, from the 54-h integrations of all sensitivity experiments.

jet, occurs near the top of the PBL in all high-resolution runs except in HUT35. This peak updraft does not seem to be related to any computational instability, because this feature still appears when the time step of 13.3 seconds for the finest 6-km resolution domain is reduced by half (i.e., 6.7 seconds); see Zhang and Wang (2003) for more details. This feature results more likely from the Ekman pumping processes, which is associated with the intense cyclonic vorticity generated by the peak tangential winds and a radial outflow jet near the top of the PBL (see Zhang et al. 2001), that are then enhanced by diabatic heating.

Fig. 7 shows the storm-scale averaged heating profiles from each sensitivity run which represent the collective effects of deep convection on the large-scale environment. These profiles exhibit a deep layer of intense latent heating up to an altitude of 13 km in the eyewall, with a bimodal heating distribution: one associated with the low-level outflow jet and the other in the upper-level outflow layer. All these are similar to those shown in Zhang et al. (2002) except for their magnitudes due to the use of different radii for the area averages. Evidently, the heating rates depend highly on the vertical resolution in the same way as the storm intensity. Namely, the higher the vertical resolution, the more intense latent heating and a stronger storm it is, since hurricanes are driven by latent heat release. The heating profiles from the other runs, particularly HRL69, are systematically much greater in magnitude than those from LRL23 and HUT35 throughout the troposphere. Again, the vertical heating profiles from Exps. LRL23 and HUT35 are almost identical in structure and magnitude; similarly among CTL46, HLT35 and HBL29 up to z = 7 km, as could be expected from their similar resolutions in the low troposphere.

While increasing the upper-level resolution has little impact on the eyewall structure, it does increase slightly the

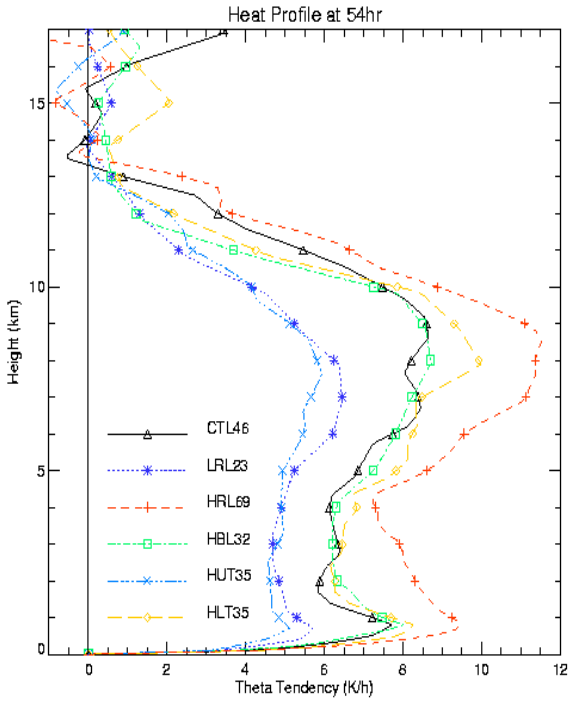


Fig. 7: Vertical profiles of the latent heating rates (K $h^{-1}$) averaged within a radius of 150 km from the 54-h integrations of all sensitivity experiments.

heating rates in the upper outflow layer (e.g., HUT35 vs. LRL23, CTL46 vs. HLT35 and HBL29). This result appears to suggest that the use of higher vertical resolution helps trigger the grid-box depositional growth (condensation) and sublimation (evaporation). For example, consider two extreme cases for a given relative humidity: a very thick and a very thin layer. The grid-box saturation will likely occur first in the thin layer if all the other conditions are identical. Of course, the decrease in truncation errors leading to the generation of stronger divergence, as the vertical resolution increases, may also contribute positively to the magnitude of latent heating and the storm intensity. Nevertheless, it is well known that the low-level heating maximum is more efficient than the upper-level one in spinning up mesoscale cyclones (Tracton 1973; Anthes and Keyser 1979; Zhang et al. 1988). The more intense low-level heating

with the increased local resolution is consistent with the increased hurricane intensity.

## 4. Summary and Conclusions

In this study, several 72-h numerical integrations are performed to study the sensitivity of the simulated Hurricane Andrew (1992) to various vertical resolutions and time-step sizes using the nested grid, cloud resolving version of the PSU/NCAR nonhydrostatic model (i.e., MM5) with the finest grid size of 6 km. The vertical resolution varies from 23 to 69 layers, with varying layer thicknesses in the lower and upper portions of the troposphere.

It is shown that changing vertical resolution has important impact on the hurricane intensity and inner-core cloud/precipitation structures. Specifically, increasing vertical resolution tends to simulate a deeper storm in terms of central pressure, three-dimensional winds with more precipitation. For the vertical resolutions tested herein, the surface central pressure could range from 932 to 899 hPa, the azimuthally averaged peak values of the tangential wind from 60 to 90 m $s^{-1}$, the PBL inflow from 30 to 40 m $s^{-1}$, the updraft from 2.5 to 4.5 m $s^{-1}$, and the diabatic heating rates from 50 to 80 K $h^{-1}$. Similarly, the low-level outflow jet and the upper-level outflow increase significantly, both nearly double as the vertical resolution increases from 23 to 69 layers. Of importance is that the deepest storm simulated could reach the maximum potential intensity calculated from the prevailing sea-surface temperature, and this trend would continue as the vertical resolution further increases, indicating that some parameterized model physical processes (e.g., cloud microphysics or the PBL) may be too sensitive to the vertical resolution.

It is found that increasing the vertical resolution in the low troposphere is more efficient in intensifying a hurricane, whereas changing the upper-level vertical resolution has little impact on the intensity prediction. The former case could cause more deepening of hurricanes because the low-level latent heating tends to induce more moisture convergence in the PBL where the latent energy source is originated. On the other hand, the increased latent heating in the upper levels would cause the convergence of the midlevel cold and dry air, suppressing deep convection in the eyewall. With higher resolutions in the low troposphere, the model produces a wider eyewall, stronger spiral rainbands and a wider area of precipitation as a result of a more intense low-level outflow jet being generated. It is shown that the noisy flows resulting from inconsistent resolutions found in the previous studies are only notable in the upper-level outflow where it is inertially less stable.

It is shown that the use of a thicker surface layer tends to produce the higher maximum surface wind; different surface layer thicknesses could produces the maximum winds ranging from 75 m $s^{-1}$ (with 80 m) to 60 m $s^{-1}$ (with 27 m). This is consistent with the notion that the frictional effects would be more (less) pronounced if a thinner (thicker) surface layer of air mass interacts with the bottom surface. This suggests that a thin surface layer be used, if possible, to verify against observations at an altimeter level (z = 10 m).

In conclusion, it is highly desirable to use higher vertical resolution when it is possible, together with higher horizontal grid resolution, to model more realistically tropical storms and the other MCSs. It should be mentioned, though, that the above conclusion may not be applicable in certain cases in which most of precipitation is generated by convective parameterization in coarse-resolution models.


### Acknowledgments

This work was supported by the NSF grant ATM-9802391, the NASA grant NAG-57842, and the ONR grant N00014-96-1-0746.

## References


Anthes, R. A., and D. Keyser, 1979: Tests of a fine-mesh model over Europe and the United States. *Mon Wea. Rev.*, **107,** 963–984.

Dudhia, J., 1989: Numerical study of convection observed during the winter monsoon experiment using a mesoscale two-dimensional model., *J. Atmos. Sci.*, **46,** 3077–3107

Dudhia, J., 1993: A nonhydrostatic version of the Penn State-NACR mesoscale model: Validation tests and simulation of an Atlantic cyclone and cold front. *Mon. Wea. Rev.*, **121,** 1493–1513

Lindzen, R. S., M. S. Fox-Rabinovitz, 1989: Consistent vertical and horizontal resolution. *Mon. Wea. Rev.,* **117,** 2575–2583

Liu, Y., D.-L. Zhang, and M.K. Yau, 1997: A Multiscale numerical study of Hurricane Andrew (1992). Part I: An explicit simulation. *Mon. Wea. Rev.*, **125,** 3073–3093

□□, □□, and □□, 1999: A Multiscale numerical study of Hurricane Andrew (1992). Part II: Kinematics and inner-core structures. *Mon. Wea. Rev.*, **127,** 2597–2616

Pecnick, M. J. and D.Keyser, 1989: The effect of spatial resolution on the simulation of upper-tropspheric frontogenesis using a sigma-coordinate primitive equation model. *Meteorol. Atoms. Phys.*, **40,** 137–149

Persson, P. O. G. and T. T. Warner, 1991:Model generation of spurious gravity waves due to inconsistency of the vertical and horizontal resolution. *Mon. Wea. Rev.*, **119,** 917–935

Tao, W.-K., and J. Simpson, 1993: The Goddard cumulus ensemble model. Part I: Model description. *Terr. Atmos. Oceanic Sci.*, **4,** 35–72

Tracton, M. S., 1973: The role of cumulus convection in the development of extratropical cyclones. *Mon. Wea. Rev.*, **107,** 572–593

Zhang, D.-L., and R. A. Anthes, 1982: A high-resolution model of the planetary boundary layer-Sensitivity tests and comparisons with SESAME-79 data. *J. Appl. Meteor.*, **21,** 1594–1609

□□, □□, 1988: A Numerical investigation of a convectively generated, inertially stable, extratropical warm-core mesovortex over land. Part I: Structure and evolution. *Mon. Wea. Rev.*, **116,** 2660–2687

□□, □□, and □□, 2002: A multiscale numerical study of Hurricane Andrew (1992). Part V: Inner-core thermodynamics. *Mon. Wea. Rev.*, **130,** 2745–2763.

□□, and X. Wang, 2003: Dependence of Hurricane intensity and structures on vertical resolution and time-step size. *Adv. Atmos. Sci.,* **20**, 711-725.